VEPP-2000 COLLIDER OPERATION IN FULL ENERGY RANGE WITH NEW INJECTOR

D. Shwartz[†1], V. Anashin, A. Batrakov, O. Belikov, D. Berkaev, D. Burenkov, K. Gorchakov,
A. Kasaev, A. Kirpotin, I. Koop[1], A. Krasnov[1], G. Kurkin, A. Lysenko, S. Motygin, A. Otboyev,
A. Pavlenko, E. Perevedentsev[1], V. Prosvetov, D. Rabusov, Yu. Rogovsky[1], A. Semenov,
A. Senchenko[1], D. Shatilov, P. Shatunov, Yu. Shatunov[1], O. Shubina, M. Timoshenko, S. Vasichev,
V. Yudin, I. Zemlyansky, Yu. Zharinov

Budker Institute of Nuclear Physics, Novosibirsk, 630090, Russia
[1]also at Novosibirsk State University, Novosibirsk, 630090, Russia

Abstract

VEPP-2000 is the only electron-positron collider operating with round beams that allow to enhance beam-beam limit. VEPP-2000 with SND and CMD-3 detectors carried out two successful data-taking runs after new BINP injection complex was commissioned. The 2016/2017 run was dedicated to high energy range (640-1000 MeV per beam) while the 2017/2018 run was focused at 275-600 MeV/beam energies. With sufficient positron production rate and upgraded full-energy booster the collider luminosity was limited by beam-beam effects, namely flip-flop effect. Thorough machine tuning together with new ideas introduced to suppress flip-flop allowed to establish new world record for beam-beam parameter and bunch-by-bunch luminosity values at specific beam energies. The achieved luminosity increased 2-5 times in a whole energy range in comparison to phase-1 operation (2010-2013).

VEPP-2000 OVERVIEW

VEPP-2000 is a small 24 m perimeter single-ring collider operating in one-by-one bunch regime in the energy range below 1 GeV per beam [1-4]. Its layout is presented in Fig. 1. Collider itself hosts two particle detectors [5, 6], Spherical Neutral Detector (SND) and Cryogenic Magnetic Detector (CMD-3), placed into dispersion-free low-beta straights. The final focusing (FF) is realized using superconducting 13 T solenoids. The main design collider parameters are listed in Table 1.

Figure 1: VEPP-2000 collider photo.

Table 1: VEPP-2000 Design Parameters (at E = 1 GeV)

Parameter	Value
Circumference, C	24.39 m
Energy range, E	150–1000 MeV
Number of bunches	1×1
Number of particles per bunch, N	1×10^{11}
Betatron functions at IP, $\beta^*_{x,y}$	8.5 cm
Betatron tunes, $\nu_{x,y}$	4.1, 2.1
Beam emittance, $\varepsilon_{x,y}$	1.4×10^{-7} m rad
Beam–beam parameters, $\xi_{x,z}$	0.1
Luminosity, L	1×10^{32} cm^{-2} s^{-1}

Injection Chain Upgrade

During commissioning and first operation phase in 2010–2013 VEPP-2000 used old positron production and injection chain that restricted available positron beam intensity and limited the luminosity at energy range above 500 MeV. Since 2016, VEPP-2000 is linked to the new BINP injection complex (IC) [7, 8] via long transfer channel. In addition, the booster BEP was upgraded in order to increase top energy up to 1 GeV and perform top-up injection [9]. Minor changes were made in addition at VEPP-2000 storage ring [10, 11].

SND and CMD-3 Physics Program

Experimental program at VEPP-2000 includes:

1. Precise measurement of R = $\sigma(e^+e^- \to$ hadrons)/ $\sigma(e^+e^- \to \mu^+\mu^-)$ to achieve less than 1% systematic for major channels. Contribution to magnetic anomaly of muon $(g$–$2)/2$ comes mainly from low energy ranges.
2. Study of exclusive hadronic channels of e^+e^- annihilation, ~ 30 channels in total.
3. Study of the "excited" vector mesons: ρ', ρ'', ω', ϕ'.
4. Study of G_E/G_M for nucleons near threshold.
5. CVC tests: comparison of isovector part of cross section to hadrons with τ-decay spectra.
6. Measurement of the cross-sections using ISR.
7. Diphoton physics, e.g. η, η' production.

† d.b.shwartz@inp.nsk.su

Round Colliding Beams

The VEPP-2000 collider exploits the round beam concept (RBC) [12]. This approach, in addition to the straight-forward geometrical gain factor in luminosity should yield the beam-beam limit enhancement. An axial symmetry of the disruptive nonlinear counter-beam force together with the X–Y symmetry of the transfer matrix between the two IPs provide an additional integral of motion, namely, the longitudinal component of angular momentum $M_z = x'y - xy'$. Although the particles' dynamics remain strongly nonlinear due to beam-beam interaction, it becomes effectively one-dimensional. The reduction of degrees of freedom thins out the resonance grid and suppress the diffusion rate resulting finally in a beam-beam limit enhancement [13].

Thus, there are several demands upon the storage ring lattice suitable for the RBC:

1. Head-on collisions (zero crossing angle).
2. Small and equal β functions at IP ($\beta^*_x = \beta^*_y$).
3. Equal beam emittances ($\varepsilon_x = \varepsilon_y$).
4. Equal fractional parts of betatron tunes ($\nu_x = \nu_x$).

The first three requirements provide the axial symmetry of collisions while requirements (2) and (4) are needed for X–Y symmetry preservation between the IPs.

Energy Calibration With CBS

For precise energy calibration of VEPP-2000 we use Compton backscattering method [14]. Laser beam meets the electron one, and backscattered photons are measured with detector (Fig. 2).
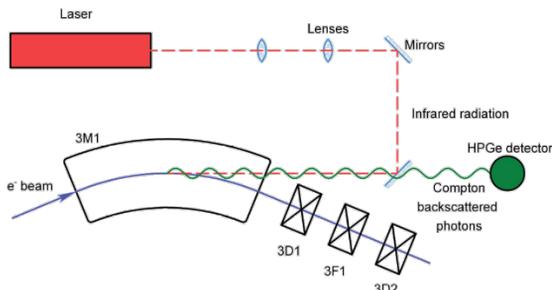

Figure 2: CBS method scheme.

Very first experiments showed scattering spectrum as shown in Fig. 3.
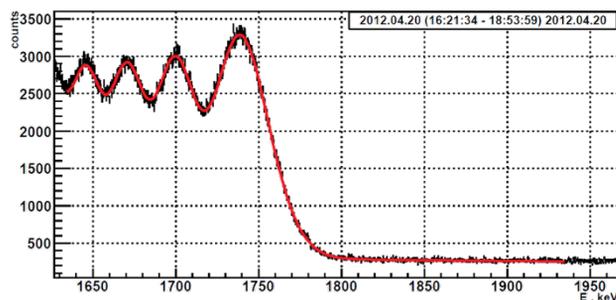

Figure 3: CBS typical spectrum edge.

An explanation was proposed based on laser beam interference from several points of interaction region. After that

these data were put in the energy calibration formula, the accuracy for the given figure is $E = 993.662 \pm 0.016$ MeV. Now the energy measurement based on CBS method is in routine operation.

Flip-Flop Effect

The final beam-beam limit at VEPP-2000 corresponds to the onset of a flip-flop effect [15]: the self-consistent situation when one of the beam sizes is blown-up while another beam size remains almost unperturbed. The simple linear model of flip-flop was discussed earlier [16], with a very high threshold intensity. Observed in VEPP-2000 behavior is most likely caused by an interplay of beam-beam interaction and nonlinear lattice resonances.

The flip-flop threshold is sensitive to several tuning knobs, in particularly to X–Y coupling and beta-functions misbalance at IP. In addition, the influence of bunch length on the threshold was observed [17].

BEAM SHAKING

While taking data at low energy range where the radiative emittance is small but significant beta-squeeze is not allowed due to the DA shrinking thus leaving mechanical aperture not fully used the possibility of emittance increase appears. It allows to increase the beam current with fixed particles density, i.e. with fixed at the threshold beam-beam parameter, and to increase luminosity linearly to beam intensity.

The idea was proposed to excite transverse emittance by frequent (in comparison to damping time) but weak (in comparison to beam size) bunch kicking (see Fig. 4). In the presence of strong nonlinear forces of colliding beam after the single kick the excited coherent oscillation decoheres very quickly thus increasing effective beam emittance. This method was probably firstly proposed and tested in 1960-s at VEP-1 collider [18].
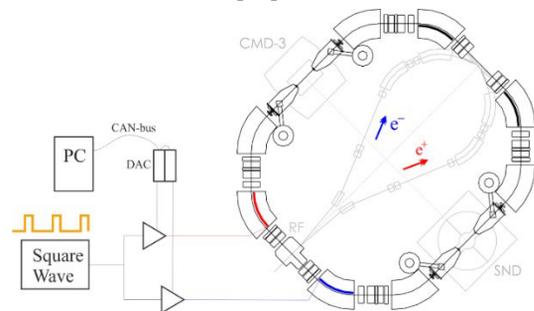

Figure 4: The scheme of beam shaking.

The typical pulses parameters are the following: pulse duration ~300 ns (3–4 turns), repetition rate $(50 \ \mu s)^{-1}$, pulse amplitude 50–100 V (depends on beam energy).

The example of beam behavior observed by pickup at 360 MeV with shaker switched on is presented in Fig. 5. Here the opposite beam is absent, kicks excite horizontal oscillations (red). One can see the fast swap to vertical oscillations (blue) due to operating at coupling resonance and relatively fast decoherence due to machine nonlinearities.

The spectrum becomes line spectrum due to presence of several kicks periodically exciting oscillations during the period of Fourier analysis.
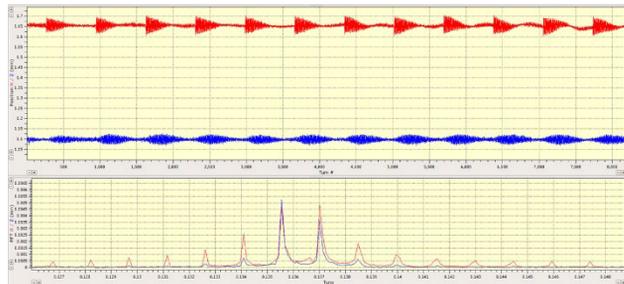

Figure 5: The signal of the single beam shaking at pickup and its Fourier spectrum.

The beam shaking in collision mode experimentally results in beams emittance growth. This growth depends on the controllable shaker parameters (pulse amplitude, pulse duration, repetition rate). The properly increased emittance prevents the flip-flop development during injection cycle: the "strong" beam can't shrink to unperturbed size when "weak" beam oscillates with large amplitudes. In addition, the beam lifetime is improved due to Touschek scattering is suppressed with increased emittance.

LUMINOSITY AND BEAM-BEAM PARAMETER

As a result of beam shaking technique implementation the beams intensities and luminosity at low energy range increased significantly. In Fig. 6 the luminosity is presented achieved in 2013 and in 2018 at the same given energy of 391–391 MeV.
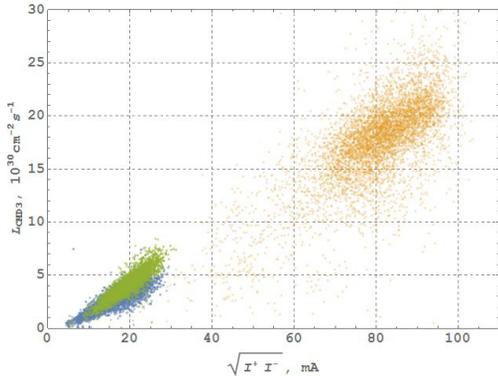

Figure 6: The CMD-3 recorded luminosity as a function of beam currents. Blue and green dots correspond to machine performance in 2013 with short and long bunch correspondingly. Yellow dots correspond to 2018.

The luminosity increased linearly with the current growth in spite of the naïve expectation of quadratic dependence from the expression for round beam:

$$L = \frac{N^+ N^-}{4\pi\sigma^{*2}} f_0,$$

that is an evidence of beam size growth driven by beam-beam interaction.

For the measured luminosity and beams intensities we can extract from latter formula the real beam size which indeed shows the linear growth with intensity (see Fig. 7).
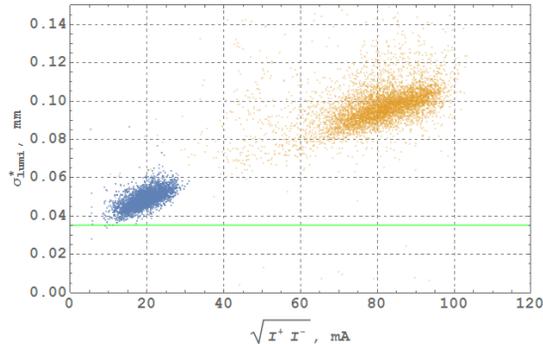

Figure 7: Beam size at IP extracted from CMD-3 luminosity. Blue and yellow dots correspond to 2013 and 2018 data. Green line shows the design beam size value.

With beam size extracted from luminosity measurements we can define the "achieved" beam-beam parameter as:

$$\xi_{\text{lumi}} = \frac{N^- r_e \beta^*_{\text{nom}}}{4\pi\gamma\sigma^{*2}_{\text{lumi}}},$$

where the beta function is nominal design value at IP. In addition, we can define "nominal" ξ in a similar way:

$$\xi_{\text{nom}} = \frac{N^- r_e \beta^*_{\text{nom}}}{4\pi\gamma\sigma^{*2}_{\text{nom}}},$$

where beam size is unperturbed. Due to strong emittance and beam size growth ξ_{nom} has nothing to do with real beam-beam tune shifts being just a beam intensity normalized to clean out the dependence on energy.

We can now express directly the luminosity via beam-beam parameter:

$$L = \frac{N f_0 \gamma}{r_e} \frac{\xi_{\text{lumi}}}{\beta^*_{\text{nom}}}.$$

Finally, the achieved beam-beam parameter extracted from luminosity at 391–392 MeV is presented in Fig. 8. It saturates strongly and doesn't exceed 0.08.
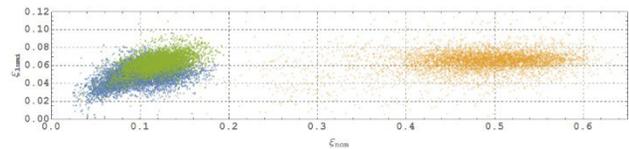

Figure 8: Beam-beam parameter extracted from CMD-3 luminosity. Notation is the same as in Fig. 6.

Coherent Modes

The cross-check for the acting beam-beam parameter value can be done through the analysis of the coherent beam oscillation spectrum [15]. In Fig. 9 the example of coherent spectrum and spectrogram at beam energy of 360 MeV are shown. Left peak corresponds to so called σ-mode with unperturbed betatron tune 0.135 while the right peak indicates the π-mode with shifted tune to 0.345. The total tune shift is $\Delta\nu = 0.21$.
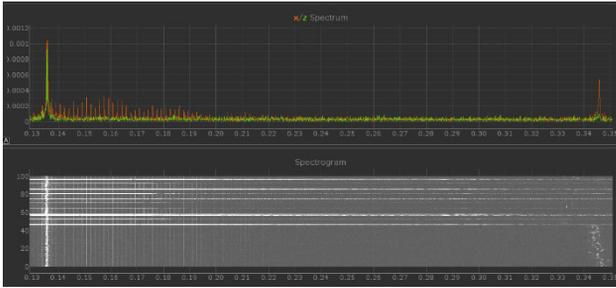
Figure 9: Beam-beam modes spectrum @ 360 MeV.

Assuming Yokoya factor [19] equal to 1 [4], with the given modes' tunes calculated ξ per one IP is equal to:

$$\xi = \frac{\cos(\pi v_\sigma) - \cos(\pi v_\pi)}{2\pi \sin(\pi v_\sigma)} \approx 0.17,$$

that is twice higher than beam-beam parameter defined from luminosity measurements. This discrepancy in not yet understood. However, the coherent tune shift is routinely used for the machine fine tuning including beamshaker amplitude and completely correlates with luminosity maximization.

DATA COLLECTION

The 2016/17 run was the first data taking VEPP-2000 run with new injector [20–23]. It was dedicated to energy range from 640 MeV to 1003.5 MeV per beam. The design top energy was exceeded in order to achieve the mass of $D^{*0}(2007)$. The run 2017/18 was dedicated to the data collection at low beam energies: 274–600 MeV.

Figure 10 presents the online status web-page during regular operation at 395.5 MeV energy in May 2018.
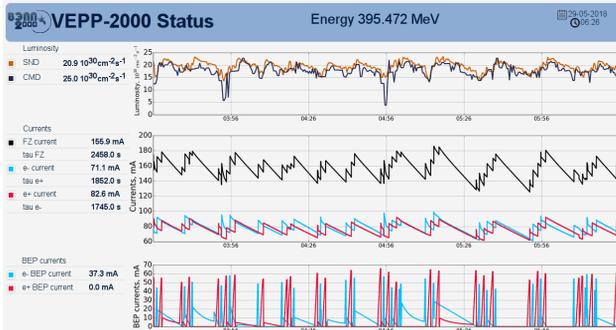

Figure 10: VEPP-2000 operation @ 395 MeV.

The achieved luminosity in comparison to 2010–2013 performance is shown in Fig. 11. In the middle energy range the achieved luminosity is well above all expectations. At the same time at top energy luminosity is lower than design value in a factor of two. The absolute record for today VEPP-2000 peak luminosity of 5×10^{31} cm^{-2}s^{-1} was achieved at the energy of 550 MeV per beam.

The next Fig. 12 presents the integrated by CMD-3 detector luminosity over all operating years since VEPP-2000 commissioning. One should beware of direct comparison of different runs integrals due to luminosity dependence on energy. 2012/13 and 2017/18 runs were spent for data taking below 500 MeV while the others were dedicated to higher energies.
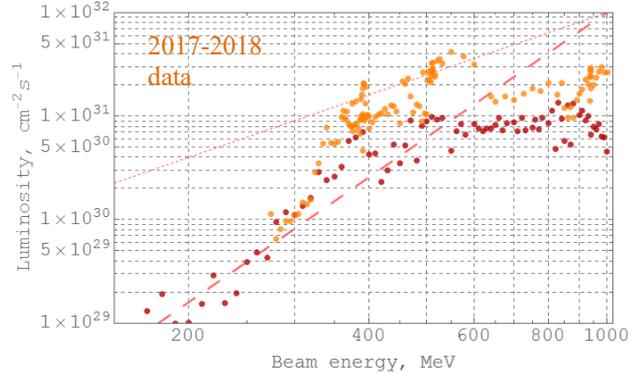

Figure 11: CMD-3 recorded in 2010–2013 (crimson) and in 2017–2018 (orange) luminosity averaged over 10% of best runs. Pink lines show scaling laws with fixed (dashed line) and variable (dotted line) β^*.
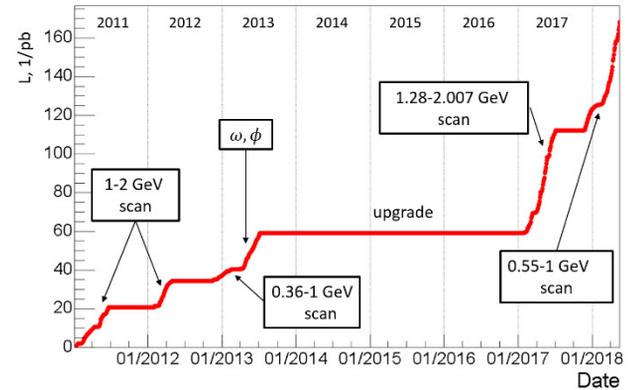

Figure 12: CMD-3 integrated luminosity by years.

The distribution of luminosity integral over energy for both particle detectors is presented in Fig. 13-14. Although all the energy range is already covered mainly integral sticks to several points of interest such as different light mesons masses [24] and threshold of nucleon-antinucleon production where the intriguing behavior of several hadrons production cross-section is observed [25].
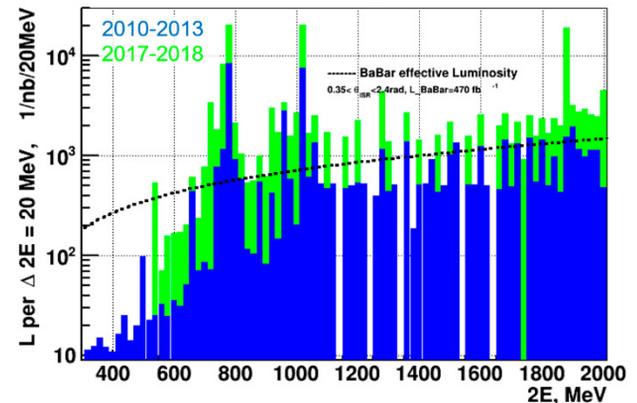

Figure 13: CMD-3 recorded luminosity integral. Blue and green colors correspond to data obtained with old and upgraded VEPP-2000 injection chain. By black dashed line the effective BaBar experiment luminosity obtained with ISR technique is shown.
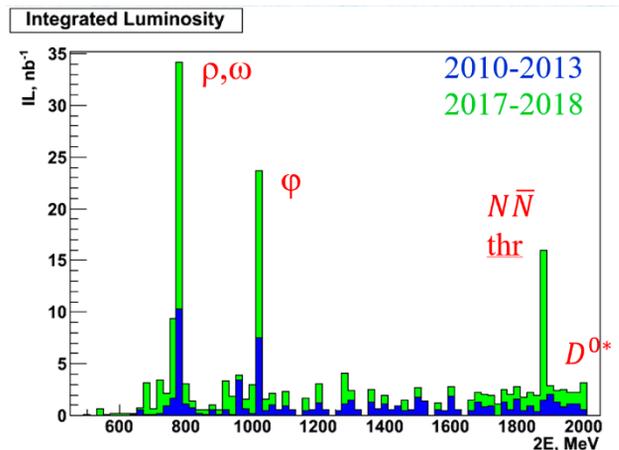
Figure 2: SND recorded luminosity integral.

CONCLUSION

CMD-3 and SND has taken more than 300 pb^{-1} of data in the whole beam energy range of $0.16 \div 1.0$ GeV with ultimate goal to take about 2 fb^{-1} in the next years. The detector subsystems upgrades are planned. New particle identification technique based on the dE/dx in 14 layers of LXe-calorimeter has been developed and will be applied in the next seasons for K^+K^-, $K^+K^-\pi^0$, $K^+K^-2\pi^0$, $K_S K^\pm\pi^\mp$ final states analyses.

Novel technique ("beamshaking") for effective emittance control allow to suppress flip-flop effect and increase beams intensity at middle energies.

ACKNOWLEDGEMENT

REFERENCES

[1] Yu. M. Shatunov *et al.*, "Project of a New Electron-Positron Collider VEPP-2000", in *Proc. EPAC'00*, Vienna, Austria (2000) pp. 439-441.

[2] D. E. Berkaev *et al.,* "The VEPP-2000 electron-positron collider: First experiments", *J. Exp. Theor. Phys.*, Vol.113, no.2, p.213 (2011).

[3] A. L. Romanov *et al.*, "Status of the Electron-Positron Collider VEPP-2000", in *Proc. NAPAC'13*, Pasadena, USA (2013) pp. 14-18.

[4] D. Shwartz *et al.*, "Round Colliding Beams at VEPP-2000 with Extreme Tuneshifts", in *Proc. eeFACT'18*, Hong Kong, China (2018) MOYBA01.

[5] A.A. Korol *et al.*, "Recent Results from the SND Detector", *Phys. Part. Nucl.* 49 (2018) no.4, pp. 730-734.

[6] R.R. Akhmetshin *et al.*, "Hadronic cross sections with the CMD-3 detector at the VEPP-2000", *Nucl. Part. Phys. Proc.*, vol. 294-296 (2018) pp. 170-176.

[7] D. Berkaev *et al.*, "VEPP-5 Injection Complex: Two Colliders Operation Experience", in *Proc. IPAC'17*, Copenhagen, Denmark (2017) pp. 2982-2984.

[8] Yu. Maltseva *et al.*, "VEPP-5 Injection Complex Performance Improvement for Two Collider Operation", in *Proc. RuPAC'18*, Protvino, Russia (2018) TUZMH02, these proceedings.

[9] D. Shwartz *et al.*, "Booster of Electrons and Positrons (BEP) Upgrade to 1 GeV", in *Proc. IPAC'14*, Dresden, Germany (2014) pp. 102-104.

[10] Yu. A. Rogovsky *et al.*, "Status and prospects of VEPP-2000 electron-positron collider", *Phys. Part. Nucl. Lett.*, 11 (2014) no.5, pp. 651-655.

[11] D. Shwartz *et al.*, "New Quadrupoles Installed at VEPP-2000 for High Energy Operation Without Final Focus", in *Proc. RuPAC'18*, Protvino, Russia (2018) WEPSB17, these proceedings.

[12] V.V. Danilov *et al.*, "The Concept of Round Colliding Beams", in *Proc. EPAC'96*, Sitges, Spain (1996) pp. 1149-1151.

[13] K. Ohmi, K. Oide and E.A. Perevedentsev, "The beam-beam limit and the degree of freedom", in *Proc. EPAC'06*, Edinburgh, Scotland, 2006, pp.616-618.

[14] E. V. Abakumova *et al.*, "A system of beam energy measurement based on the Compton backscattered laser photons for the VEPP-2000 electron–positron collider", *Nucl. Instrum. Meth. A,* vol. 744, pp. 35-40, 2014.

[15] D. Shwartz *et al.*, "Recent Beam-Beam Effects at VEPP-2000 and VEPP-4M", in *Proc. ICFA Mini-Workshop on Beam-Beam Effects in Hadron Colliders (BB2013)*, Geneva, Switzerland, 2013, CERN-2014-004, pp. 43-49.

[16] A.V. Otboyev and E.A. Perevedentsev. "On self-consistent β-functions of colliding bunches", in *Proc. PAC'1999*, New York, USA, 1999, pp. 1524-1526.

[17] D. Shwartz *et al.*, "Recent Beam-beam Effects and Luminosity at VEPP-2000", in *Proc. IPAC'14*, Dresden, Germany (2014), pp. 924-927.

[18] G.M. Tumaikin, private communication.

[19] K. Yokoya, H. Koiso, "Tune Shift of Coherent Beam-Beam Oscillations", *Particle Accelerators,* 1990, Vol.27, pp. 181-186.

[20] D. Berkaev *et al.*, "Commissioning of Upgraded VEPP-2000 Injection Chain", in *Proc. IPAC'16*, Busan, Korea (2016) pp. 3811-3813.

[21] D. Shwartz *et al.*, "Recomissioning and Perspectives of VEPP-2000 e+e− Collider", *PoS ICHEP2016* (2016), p.054.

[22] P. Shatunov *et al.*, "High Luminosity at VEPP-2000 Collider With New Injector", in *Proc. IPAC'17*, Copenhagen, Denmark (2017) pp. 2989-2991.

[23] Yu. M. Shatunov *et al.*, "Commissioning of the Electron-Positron Collider VEPP-2000 after the Upgrade", *Phys. Part. Nucl. Lett.*, 15 (2018) no.3, pp. 310-314.

[24] E.A. Kozyrev *et al.*, "Study of the process e$^+$e$^-$ → K$^+$K$^-$ in the center-of-mass energy range 1010–1060 MeV with the CMD-3 detector", *Phys. Lett. B,* 779 (2018) pp. 64-71.

[25] R. R. Akhmetshin *et al.*, "Observation of a Fine Structure in e$^+$e$^-$ → Hadrons Production at the Nucleon-Antinucleon Threshold" (2018) arXiv:1808.00145.